



HAL
open science

A method for detection of known sources of continuous gravitational wave signals in non-stationary data

P Astone, S D Antonio, S Frasca, C Palomba

► **To cite this version:**

P Astone, S D Antonio, S Frasca, C Palomba. A method for detection of known sources of continuous gravitational wave signals in non-stationary data. *Classical and Quantum Gravity*, 2010, 27 (19), pp.194016. 10.1088/0264-9381/27/19/194016 . hal-00629995

HAL Id: hal-00629995

<https://hal.science/hal-00629995>

Submitted on 7 Oct 2011

HAL is a multi-disciplinary open access archive for the deposit and dissemination of scientific research documents, whether they are published or not. The documents may come from teaching and research institutions in France or abroad, or from public or private research centers.

L'archive ouverte pluridisciplinaire **HAL**, est destinée au dépôt et à la diffusion de documents scientifiques de niveau recherche, publiés ou non, émanant des établissements d'enseignement et de recherche français ou étrangers, des laboratoires publics ou privés.

A method for detection of known sources of continuous gravitational wave signals in non-stationary data

P. Astone¹, S. D' Antonio², S. Frasca^{1,3}, C. Palomba¹

¹ INFN Roma; ² INFN Roma2; ³ Dip. di Fisica, Univ. di Roma "Sapienza"

Abstract. A method for searching continuous gravitational wave (g.w.) signals from isolated neutron stars whose position, frequency and frequency evolution are known is described in this paper. This method is applied to data of interferometric detectors such as Virgo. The method is based on the use of 5-vectors, which are the Fourier components of the signal and data at five frequencies around the source intrinsic frequency. The main characteristic of the method is its simplicity and the strong reduction of the computing time needed for the analysis and in particular for all the simulation procedures. We introduce here also the concept of "coherence" to state the reliability of a detection.

Pacs. numbers: 04.80Nn,07.05Kf,97.60Jd

1. Introduction: the formulation of the problem

Continuous g.w. signals emitted by asymmetric rotating neutron stars are an important target for interferometric detectors. In the targeted search for known sources of this kind, where "known" indicates objects like the Crab or Vela pulsar, whose position, frequency and frequency evolution are known, we have two different problems: detection of a signal whose polarization parameters are known (2 degrees of freedom (d.o.f.) problem) and detection of a signal whose polarization parameters are not known (4 d.o.f. problem). In the first case, once the signal has been detected, we should estimate the amplitude and the phase of the wave. In the second case we should estimate also the two polarization parameters. Various methods have been developed for this kind of search, see e.g. [1],[2]. We describe here a method based on the description of the signal and of the data in the domain of their five Fourier components at the five frequencies $\omega_0, \omega_0 \pm \Omega, \omega_0 \pm 2\Omega$, where ω_0 is the signal intrinsic angular frequency and Ω is the Earth sidereal angular frequency [3]. The data of an interferometer like Virgo are characterized by a sensitivity which allows interesting analysis for g.w. in the range from 10 Hz up to roughly 4kHz. The search method presented here uses only a small band around the expected signal frequency. Searching signals in non stationary data requires to prepare the data as explained in Sec. 2.

2. Preparation of the data

The preparation of the data has been discussed in detail in [4], so here we will only recall some basic features. First of all, let us point out that a basic tool we need for the analysis is the Fourier transform, which we compute using the Fast Fourier Transform

implementation (FFT). We start with the construction of a cleaned data base of FFTs, which is a collection of FFTs built from short (1024 s) chunks of calibrated data, overlapped by half. These FFTs are constructed using the whole detector band and have an header with information relevant to the analysis (e.g. the beginning time of that FFT, the window used ...). This data organization is simple and is used not only for the present coherent search.

The use of a cleaning procedure is important, and it has been developed in such a way to veto only times where disturbances act and not entire data chunks. The effect of the cleaning depends on the nature of the data, and is related to the detector characteristics in the particular considered run. And, even at the same time, it is different when considering different frequency bands. Once decided a particular source to look for we proceed with the extraction of a small band, covering a fraction of Hz, around the expected source frequency at the time of the analysis. The band extraction can be done in different ways; the one we use is based on the construction of the so-called “analytical signal” (see [5] and references therein). The analytical signal is complex and has a sampling rate much lower than the original one (typically 1 second), and it has the property that its power spectrum in the selected band is identical to the original power spectrum in that band. Then, given the known position of the source and proper ephemerides for the detector position and velocity it is possible to remove the Doppler effect, due to the Earth motion, the Einstein effect and also the effect of the source spin-down. The correction has to be very accurate, since the integration time of the search might be very long and even very small errors can sum up to unacceptable values. For this reason a procedure, based on oversampling the data, by a factor such to have at least 8 samples for each source period, and on re-sampling, which consists in the construction of a new time abscissa, as originally proposed in [6], has been developed. In a forthcoming paper we will give details on this part of the analysis method. Then, there is a further cleaning step to remove residual noisy periods, which is based a robust estimation of the noise parameters and is described in [7]. A final Wiener filter, which basically is a weight on the data, with the inverse of their local variance, reduces the impact of non-stationary noise. At this point, the g.w. signal present into the data would be monochromatic with a residual amplitude and phase modulation due to the effect of detector response, as described in Sec. 4.

For clarity, in the paper we have indicated tensors in gothic and 5-vectors in bold. If A is a complex quantity, A' is the complex conjugate. The product of vectors is always the scalar product[‡].

3. The periodic wave

The continuous g.w. signal emitted by a generic rotating rigid star can be described by a polarization ellipse. The polarization ellipse is characterized by the ratio $\eta = \frac{b}{a}$ of its semi-minor to its semi-major axis and by the angle ψ defining the direction of the major axis a respect to the celestial parallel of the source (counterclockwise). The ratio η varies in the range $[-1, 1]$, where $\eta = 0$ for a linearly polarized wave and $\eta = \pm 1$ for a circularly polarized wave ($\eta = 1$ if the circular rotation is counterclockwise). For a monochromatic signal with angular frequency ω_0 the metric perturbation tensor can be expressed as

$$\mathfrak{h}(t) = h_0 (H_+ \mathbf{e}_\oplus + H_\times \mathbf{e}_\otimes) e^{j(\omega_0 t + \gamma)} \quad (1)$$

[‡] we recall that if \mathbf{a} and \mathbf{b} are complex vectors their scalar product is $\mathbf{a} \cdot \mathbf{b} = \sum_i a_i b'_i$

where \mathbf{e}_\oplus and \mathbf{e}_\otimes are the two basis polarization tensors and the *plus* and *cross* amplitudes are given by

$$H_+ = \frac{\cos 2\psi - j\eta \sin 2\psi}{\sqrt{1 + \eta^2}} \quad (2)$$

$$H_\times = \frac{\sin 2\psi + j\eta \cos 2\psi}{\sqrt{1 + \eta^2}} \quad (3)$$

The two complex amplitudes satisfy the condition $|H_+|^2 + |H_\times|^2 = 1$. We can reverse the previous equations to express η , ψ as a function of H_+ , H_\times . This can be done using combinations of the two amplitudes which do not depend on the absolute phase γ . For instance, introducing the quantities

$$H_+ H'_\times = \frac{1 - \eta^2}{1 + \eta^2} \frac{1}{2} \sin 4\psi + j \frac{-\eta}{1 + \eta^2} = A + jB \quad (4)$$

$$|H_+|^2 - |H_\times|^2 = \frac{1 - \eta^2}{1 + \eta^2} \cos 4\psi = C \quad (5)$$

we immediately find

$$\eta = \frac{-1 + \sqrt{1 - 4B^2}}{2B} \quad (6)$$

$$\cos 4\psi = \frac{C}{(2A)^2 + C^2} \quad (7)$$

$$\sin 4\psi = \frac{2A}{(2A)^2 + C^2} \quad (8)$$

Formally identical relations will be used to estimate the unknown source parameters from the estimation of H_+ , H_\times , see Sec. 8.

4. The detector response

The gravitational wave strain at the detector is

$$h(t) = h_0 (A_+ H_+ + A_\times H_\times) e^{j(\omega_0 t + \gamma)} \quad (9)$$

where (see, e.g., [3])

$$\begin{aligned} A_+ &= a_0 + a_{1c} \cos \Omega t + a_{1s} \sin \Omega t + a_{2c} \cos 2\Omega t + a_{2s} \sin 2\Omega t \\ A_\times &= b_{1c} \cos \Omega t + b_{1s} \sin \Omega t + b_{2c} \cos 2\Omega t + b_{2s} \sin 2\Omega t \end{aligned} \quad (10)$$

where the Earth sidereal angular frequency Ωt can be expressed in terms of the local sidereal time Θ , the source right ascension α and the detector longitude β : $\Omega t = \Theta - \alpha + \beta$. The coefficients in Eq. 10 are

$$\begin{aligned} a_0 &= -\frac{3}{16}(1 + \cos 2\delta)(1 + \cos 2\lambda) \cos 2a \\ a_{1c} &= -\frac{1}{4} \sin 2\delta \sin 2\lambda \cos 2a \\ a_{1s} &= -\frac{1}{2} \sin 2\delta \cos \lambda \sin 2a \\ a_{2c} &= -\frac{1}{16}(3 - \cos 2\delta)(3 - \cos 2\lambda) \cos 2a \\ a_{2s} &= -\frac{1}{4}(3 - \cos 2\delta) \sin \lambda \sin 2a \end{aligned} \quad (11)$$

$$\begin{aligned}
 b_{1c} &= -\cos \delta \cos \lambda \sin 2a \\
 b_{1s} &= \frac{1}{2} \cos \delta \sin 2\lambda \cos 2a \\
 b_{2c} &= -\sin \delta \sin \lambda \sin 2a \\
 b_{2s} &= \frac{1}{4} \sin \delta (3 - \cos 2\lambda) \cos 2a
 \end{aligned} \tag{12}$$

where δ is the source declination, λ and a are respectively the detector latitude and azimuth.

As shown by Eq. 9, $h(t)$ is the product of two terms: the first, $(A_+H_+ + A_\times H_\times)$, is a “slow” amplitude and phase modulation at the sidereal frequency, as can be seen from Eq. 10, while the second, $e^{j(\omega_0 t + \gamma)}$, is a “fast” term, due to the intrinsic source frequency.

5. The signal 5-vect

As can be immediately seen from Eqs. 9,10, the signal in the detector is completely defined by its Fourier components at the five frequencies $\omega_0, \omega_0 \pm \Omega, \omega_0 \pm 2\Omega$ and can be, then, described in terms of a five component complex vector, which we call the *signal 5-vect*. Let us introduce a *generator 5-vect*, \mathbf{W}^* , with components

$$\mathbf{W}_k^* = e^{-jk\Omega t} = \mathbf{W}_k e^{+jk(\alpha-\beta)} \tag{13}$$

where

$$\mathbf{W}_k = e^{-jk\Theta} \tag{14}$$

with $-2 \leq k \leq 2$. The generator extracts the five Fourier components of the signal at the frequencies $\omega_0 - 2\Omega, \omega_0 - \Omega, \omega_0, \omega_0 + \Omega, \omega_0 + 2\Omega$. The signal in the detector, Eq. 9, can then be re-written as

$$h(t) = h_0 \mathbf{A} \cdot \mathbf{W} e^{j(\omega_0 t + \gamma)} \tag{15}$$

where

$$\mathbf{A} = H_+ \mathbf{A}^+ + H_\times \mathbf{A}^\times \tag{16}$$

is the *signal 5-vect*. It is a combination of the two complex amplitudes H_+, H_\times with the $+$ and \times 5-vects, $\mathbf{A}^+, \mathbf{A}^\times$, which have components

$$\begin{aligned}
 A_{-2}^+ &= \left(\frac{a_{2c}}{2} + j \frac{a_{2s}}{2} \right) e^{j2(\alpha-\beta)} \\
 A_{-1}^+ &= \left(\frac{a_{1c}}{2} + j \frac{a_{1s}}{2} \right) e^{j(\alpha-\beta)} \\
 A_0^+ &= a_0 \\
 A_1^+ &= \left(\frac{a_{1c}}{2} - j \frac{a_{1s}}{2} \right) e^{-j(\alpha-\beta)} \\
 A_2^+ &= \left(\frac{a_{2c}}{2} - j \frac{a_{2s}}{2} \right) e^{-j2(\alpha-\beta)}
 \end{aligned} \tag{17}$$

$$\begin{aligned}
 A_{-2}^\times &= \left(\frac{b_{2c}}{2} + j \frac{b_{2s}}{2} \right) e^{j2(\alpha-\beta)} \\
 A_{-1}^\times &= \left(\frac{b_{1c}}{2} + j \frac{b_{1s}}{2} \right) e^{j(\alpha-\beta)} \\
 A_0^\times &= 0 \\
 A_1^\times &= \left(\frac{b_{1c}}{2} - j \frac{b_{1s}}{2} \right) e^{-j(\alpha-\beta)} \\
 A_2^\times &= \left(\frac{b_{2c}}{2} - j \frac{b_{2s}}{2} \right) e^{-j2(\alpha-\beta)}
 \end{aligned} \tag{18}$$

It can be easily shown that both the terms $\mathbf{A}^+ \cdot \mathbf{W}$ and $\mathbf{A}^\times \cdot \mathbf{W}$ are real: thus $h(t)$ is the complex linear combination of two real functions. It can also be seen that the product $\mathbf{A} \cdot \mathbf{W}$ is real only in the case of linear polarization and, in this case, the signal is modulated only in amplitude.

6. The data 5-vect

We need to introduce also a 5-vect for the data, that is noise plus, possibly, a signal. At the output of the detector we have:

$$x(t) = h(t) + n(t) \quad (19)$$

which, in terms of the five Fourier components, becomes the *data 5-vect*

$$\mathbf{X} = \int_T x(t) \mathbf{W} e^{-j\omega_0 t} dt = h_0 e^{j\gamma} \mathbf{S} + \mathbf{N} \quad (20)$$

where T is the observation time and

$$\mathbf{S} = \int_T s(t) \mathbf{W} e^{-j\omega_0 t} dt \quad (21)$$

with $s(t) = \frac{h(t)}{h_0 e^{j\gamma}}$. \mathbf{S} is the “empirical” computation of the signal 5-vect \mathbf{A} , which theoretical components have been written in Eqs. 17 and 18, scaled by a factor which is proportional to the observation time. In absence of a signal, the noise 5-vect would be

$$\mathbf{N} = \int_T n(t) \mathbf{W} e^{-j\omega_0 t} dt \quad (22)$$

obtained from the data extracting the five Fourier components at the frequencies $\omega_0 + k\Omega$, $k = -2, \dots, 2$. A data 5-vect has 10 d.o.f. (5 independent complex components).

6.1. The 5-vector \mathbf{S} versus \mathbf{A} : empirical construction of 5-vects

The construction of the signal 5-vect \mathbf{S} is “empirical” and this is a very important point of the method. As will be described in Sec. 7, the detection of the signal in the 4 d.o.f. case is based on the construction of a filter matched to the signal + and \times components: if these components were obtained using Eqs. 17 and 18, the matching condition would not take into account the presence of holes in the data and the effect of all the operations done on the data, such as cleaning or Wiener weighting. Then, in practice we simulate in time domain the signal + and \times components, which depend only on the source and detector position, with an arbitrary amplitude, and we obtain the time vectors $s_+(t)$, $s_\times(t)$. We then operate on them with all the procedures used for the data and compute the corresponding empirical 5-vect \mathbf{S}_+ , \mathbf{S}_\times by using Eq. 21. In the 2 d.o.f. we need to compute just one “empirical” 5-vect \mathbf{S} , see Sec. 7.1.

Given the finite duration of the Fourier transform in Eq. 21 part of the energy of the Fourier components will be spread into lateral bands. We checked that the energy we loose for this reason is less than (1-2) % in all practical cases we met in the analysis.

7. The detection

In the following we will always refer to the signal 5-vect as \mathbf{A} , but all the equations are valid, and applied in practice, to its empirical realization \mathbf{S} .

7.1. 2 d.o.f case

This is the case when we know the two polarization parameters, η , ψ , and we want to detect the signal and estimate its amplitude and phase. The shape of the signal is known and the matched filter theory can be used. Given \mathbf{X} , the 5-vec of the data, and \mathbf{A} , the 5-vec of the signal, the matched filter transfer function is $\frac{\mathbf{A}'}{|\mathbf{A}|^2}$. The filter output is the estimation of the signal complex amplitude:

$$\hat{h} = \widehat{h_0 e^{j\gamma}} = \frac{\mathbf{X} \cdot \mathbf{A}}{|\mathbf{A}|^2} \quad (23)$$

7.2. 4 d.o.f case

In this case we don't know the polarization parameters and thus the detection can't be done using the matched filter theory, as we don't know the relative weight of the plus and cross components of the signal, i.e. we don't know its shape. In fact we can only estimate the two observables

$$\hat{h}_+ = \frac{\mathbf{X} \cdot \mathbf{A}^+}{|\mathbf{A}^+|^2}; \quad \hat{h}_\times = \frac{\mathbf{X} \cdot \mathbf{A}^\times}{|\mathbf{A}^\times|^2} \quad (24)$$

They are the estimation, respectively, of the amplitudes $h_0 e^{j\gamma} \cdot H_+$, $h_0 e^{j\gamma} \cdot H_\times$.

7.3. The detection statistics

To construct a detection statistics we have to use the two basic observables of Eq. 24.

Let us introduce the following detection statistics:

$$S = c_+ |\hat{h}_+|^2 + c_\times |\hat{h}_\times|^2. \quad (25)$$

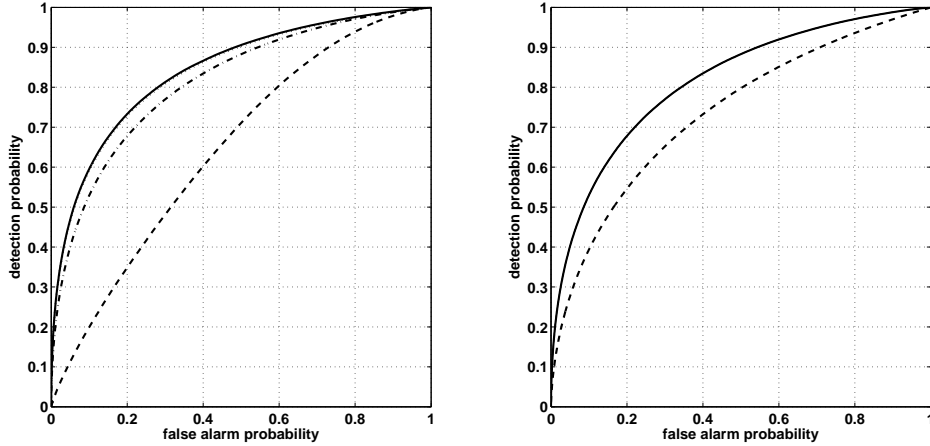


Figure 1. ROC curves for different detection statistics: simple mean (dashed line), F-stat (dot-dashed), best ROC (continuous), best SNR (dotted). We notice that in each graph some of these curves -not always the same- are superposed. Left: ratio of the two modes $\frac{|\mathbf{A}^+|}{|\mathbf{A}^\times|} = 3$. Right: ratio of the two modes $\frac{|\mathbf{A}^+|}{|\mathbf{A}^\times|} = 1$. The latter is approximately the situation we have for the Vela pulsar.

The coefficients of the linear combination in Eq. 25 can be chosen to fulfill different requirements. We have studied some situations, which we think are more significant, and compared them by computing the corresponding ROC curves, i.e. the detection probability as a function of the false alarm probability. A simple choice is to take the two coefficients equal, which means to take the simple mean: $c_+ = c_\times = \frac{1}{2}$. If we take the two coefficients proportional to the square of the absolute values of the signal 5-vectors,

$$c_+ = |\mathbf{A}^+|^2, \quad c_\times = |\mathbf{A}^\times|^2$$

we have the well known F-statistics [8], which is an equalization of the response at the two modes. Another possible choice is to take the two coefficients proportional to the 4th power of the absolute values of the signal 5-vectors

$$c_+ = |\mathbf{A}^+|^4, \quad c_\times = |\mathbf{A}^\times|^4$$

This corresponds to weight more the most sensitive mode (we call this choice “best ROC”, see later). The last choice we consider is to take only the most sensitive mode (one weight is 1 and the other is 0); it can be demonstrated that this produces the highest output SNR (we call this “best SNR”).

We have performed a set of simulations and computed the ROC curves for the four cases we considered, and considering several values of the ratio $\frac{|\mathbf{A}^+|}{|\mathbf{A}^\times|}$ between the + and × modes. Results are plotted in Fig. 1 for two different ratios of the two modes: $\frac{|\mathbf{A}^+|}{|\mathbf{A}^\times|} = 1$ (right plot), $\frac{|\mathbf{A}^+|}{|\mathbf{A}^\times|} = 3$ (left plot), and taking the input signal-to-noise ratio $SNR = 1.5$. Left plot shows that the use of coefficients proportional to $|\mathbf{A}^{+, \times}|^4$ is the best choice in that case, with the “best snr” statistic which is just slightly worse. Right plot shows that in some particular cases, like this in which the two modes have the same weight, apart from the simple mean the other statistics are basically equivalent.

Even if it is not evident from the figure, let us comment that we have analyzed many different sets of parameters, obtaining in all cases that the choice $c_{+, \times} = |\mathbf{A}^{+, \times}|^4$ is the best.

8. Estimation of the source parameters

Starting from \hat{h}_+ and \hat{h}_\times , see Eq. 24, we can estimate the signal four parameters. The estimation of the amplitude at the detector is

$$\hat{h}_0 = \sqrt{|\hat{h}_+|^2 + |\hat{h}_\times|^2} \quad (26)$$

To estimate η , ψ , similarly to what has been done in Sec. 3, we may write

$$\hat{h}_+ \hat{h}'_\times = A + jB \quad (27)$$

$$|\hat{h}_+|^2 - |\hat{h}_\times|^2 = C \quad (28)$$

and we get, formally, the same results as in Eqs. 6, 7, 8:

$$\hat{\eta} = \frac{-1 + \sqrt{1 - 4B^2}}{2B} \quad (29)$$

$$\cos 4\hat{\psi} = \frac{C}{(2A)^2 + C^2} \quad (30)$$

$$\sin 4\hat{\psi} = \frac{2A}{(2A)^2 + C^2} \quad (31)$$

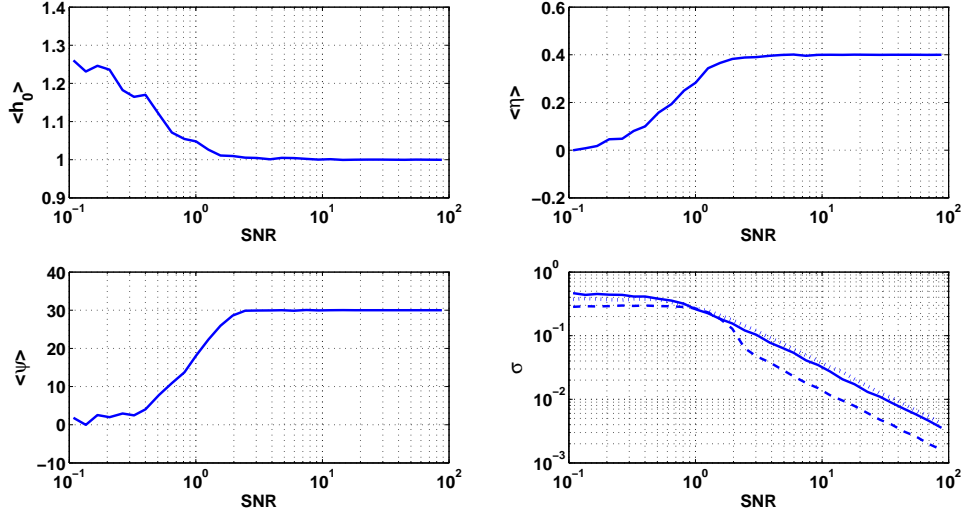


Figure 2. Accuracy and precision in parameter estimation. The two top and the bottom left plots show, as a function of SNR, the mean value of the estimation of h_0 (normalized to the injected value), η and ψ obtained in a Monte Carlo simulation. In this example the injected signals had parameters $\psi = 30^\circ$ and $\eta = 0.4$ and came from the direction of the Vela pulsar. The bottom right plot shows the standard deviation of the estimation for h_0 (continuous line), η (dotted line), ψ (dashed line).

The estimation of the initial phase γ is obtained from

$$e^{j\hat{\gamma}} = \frac{\hat{h}_+}{H_+(\hat{\eta}, \hat{\psi})} = \frac{\hat{h}_\times}{H_\times(\hat{\eta}, \hat{\psi})} \quad (32)$$

We have performed simulations by injecting signals in gaussian noise to study the characteristic of the estimators. In particular, Fig. 2 shows the average value and standard deviation of the estimation of h_0 (normalized to the injected value), η and ψ as a function of the SNR taking $\psi = 30^\circ$ and $\eta = 0.4$ for the injected signals and assuming they come from the direction of the Vela pulsar. Very similar results are obtained for different values of the parameters.

We notice that for $\text{SNR} > 2$ the estimation is good in all cases: the estimators are unbiased and the precision of the estimation increases linearly with the SNR.

9. The reliability of the detection: the coherence

Once a detection has been done, we characterize its reliability by introducing a parameter, which we call the “coherence”, defined as

$$c = \frac{|\hat{h}\hat{\mathbf{A}}|^2}{|\mathbf{X}|^2}; \quad 0 \leq c \leq 1 \quad (33)$$

where, in the 4 d.o.f case, $\hat{\mathbf{A}} = \hat{h}_+ \mathbf{A}_+ + \hat{h}_\times \mathbf{A}_\times$ is the estimated signal 5-vect, \hat{h} is the estimated complex amplitude and \mathbf{X} the data 5-vect. In the 2 d.o.f case we simply

have $\hat{\mathbf{A}} = \mathbf{A}$. If we introduce the normalized 5-vectors, $\tilde{\mathbf{X}} = \frac{\mathbf{X}}{|\mathbf{X}|}$, $\tilde{\mathbf{A}} = \frac{\hat{\mathbf{A}}}{|\hat{\mathbf{A}}|}$, and since $\hat{h} = \frac{\mathbf{X} \cdot \hat{\mathbf{A}}}{|\hat{\mathbf{A}}|^2}$, we can write

$$c = |\tilde{\mathbf{X}} \cdot \tilde{\mathbf{A}}|^2 \quad (34)$$

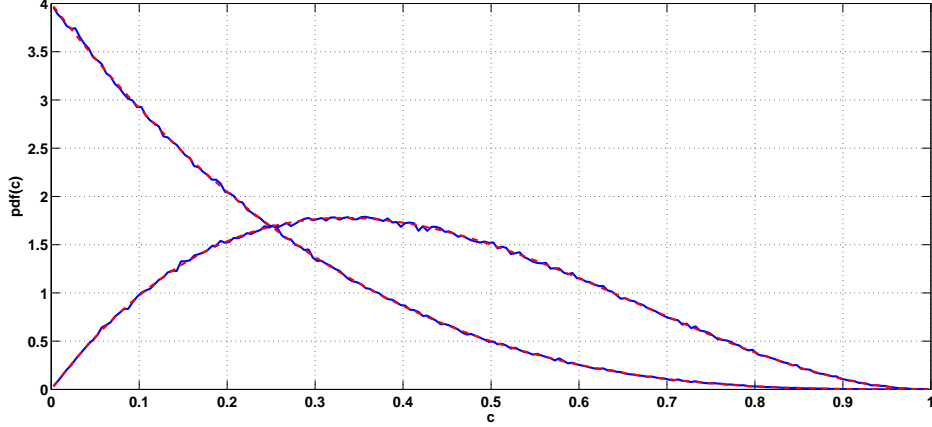


Figure 3. Probability density functions for the coherence (both theoretical and obtained from simulations) for the 2 d.o.f. case (monotonic functions) and the 4 d.o.f case.

which does not depend on the amplitudes of both \mathbf{X} and $\hat{\mathbf{A}}$. The coherence here is a number (between 0 and 1) which measures the resemblance among the shape of the expected signal and the data. In fact it does not depend on scaling factors on the signal, but only on its shape. Using simulations we have numerically found that, in the absence of signals, the coherence is distributed according to a β distribution.

$$2 \text{ d.o.f. : } f(c) = 4 \cdot (1 - c)^3 \quad (35)$$

$$4 \text{ d.o.f. : } f(c) = 12 \cdot c \cdot (1 - c)^2 \quad (36)$$

In Fig. 3 the distributions of the coherence (both theoretical and obtained from simulations) are shown. We see that the use of the coherence gives more stringent constraints in the 2 d.o.f. case than in the 4 d.o.f case in the sense that it is harder to get higher values of coherence with only noise in the 2 d.o.f. case. The properties and the use of the coherence will be discussed in detail in a forthcoming paper.

10. Considerations on the application to real data

The method has been developed having in mind the real characteristics of interferometric g.w. detectors. Indeed, as explained in Sec. 2, an important part of the pipeline has been designed to take into account non-stationarities and disturbances present in the data. Also the detection procedure, see Sec. 7 on the construction of the “empirical” 5-vectors, has been designed to work with real data taking properly into account the presence of holes and other non-stationarities.

The analyzed data are always characterized by an uncertainty, both in amplitude and in phase, due to the calibration and reconstruction procedures. These errors,

which typically vary with frequency, are not under our direct control, and they will influence the analysis results. A scaling factor on the reconstructed data will influence the estimation of an upper limit or the estimation of the amplitude of the signal. The error on the phase will just affect the estimation of the absolute phase (unless it significantly changes over a band of the order of 10^{-5} Hz, something which normally does not happen). In typical data taking runs the relative error in amplitude amounts to a few percent and the error in phase to a few tens of *mrاد*.

11. Advantages of the use of the 5-vect formalism

There are several advantages in using the 5-vect formalism. First of all the application of a matched filter, see Sec. 7, consists in the scalar product between 2 complex vectors each with five components. On the contrary, the application of a matched filter between a time domain signal and a time domain template, this is what is done typically, implies a scalar product among two vectors with $O(10^7)$ components (assuming a sampling rate of 1 Hz and an observation time of 10^7 s). Then we have a computational gain of $O(10^6)$ respect to the classical application of the matched filter. This gain is particularly important when several (thousand or tens of thousand) simulated signals must be generated and analyzed to make studies of detection efficiency or to set upper limit on signal amplitude. Another advantage of this formalism is that the signal 5-vects do not depend on frequency. As a consequence it is straightforward, and computationally cheap, to extend the search to a band of frequencies (i.e. taking into account the possibility that the g.w. signal frequency is not simply twice the source angular frequency). Moreover, also the extension to multiple detectors is immediate. These last two issues will be discussed in a forthcoming paper.

Conclusions

We have presented a method we are using to analyze Virgo data to search for known sources of continuous g.w., such as the Vela pulsar. At its hearth there is the idea of 5-vector, i.e. a complex vector which five components are the data or signal Fourier components at the source intrinsic angular frequency ω_0 and at $\omega_0 \pm \Omega$, $\omega_0 \pm 2\Omega$, being Ω the Earth sidereal angular frequency. The method is, according to us, particularly interesting as it is very simple and drastically reduces the computational time needed for the analysis, in particular when multiple signal injections are needed to evaluate statistics or upper limits. The use of 5-vects makes simple the extension of the method for the analysis of a wider frequency band, for the analysis of data from more detectors and for the analysis done dividing the observation time into sub-periods, which can be useful in some cases to enhance the reliability of the detection.

Appendix A

We have computed the relation among the description of the wave we are using, see Eq. 1, and the description, widely used in the community, of the wave emitted from a non axi-symmetric neutron star, rotating around a principal axis of inertia. The parameters used in this formalism, see e.g. [1], are the two mode amplitudes

$$a_+ = a_0 \frac{1 + \cos^2 \iota}{2}; \quad a_\times = a_0 \cos \iota \quad (37)$$

where ι is the angle between the pulsar rotation axis and the direction of the detector. The amplitude at the detector which we use, h_0 , is related to a_+ , a_\times by

$$h_0 = \sqrt{a_+^2 + a_\times^2} \quad (38)$$

Combining the above equations we have

$$h_0 = a_0 \sqrt{\frac{1 + 6\cos^2\iota + \cos^4\iota}{4}} \quad (39)$$

It is also straightforward to show that the relation between η and the angle ι is given by

$$\eta = -\frac{2\cos\iota}{1 + \cos^2\iota} = -\frac{a_\times}{a_+} \quad (40)$$

Bibliography

- [1] R. J. Dupuis, G. Woan “Bayesian estimation of pulsar parameters from gravitational wave data” PRD 72, 102002 (2005)
- [2] P. Jaranowski, A. Krolak, B.F. Schutz, Phys. Rev. D 58, 063001 (1998)
- [3] S. D’ Antonio, S. Frasca, C. Palomba “Spectral filtering for c.w. searches” CQG, 26, No 20, 204012 (2009)
- [4] The Virgo collaboration “Cleaning the Virgo sampled data for the search of periodic sources of gravitational waves”, CQG, 26 No 20, 204002 (2009)
- [5] P. Astone, M. Bassan, P. Bonifazi, P. Carelli, E. Coccia, C. Cosmelli, S. D’ Antonio, V. Fafone, S. Frasca, Y. Minenkov, I. Modena, G. Modestino, A. Moleti, G.V. Pallottino, M. A. Papa, G. Pizzella, L. Quintieri, F. Ronga, R. Terenzi, M. Visco, “Search for periodic g.w. sources with the Explorer detector”, Phys Rev D 65,022001 (2002)
- [6] J. Livas “Broadband search techniques for periodic sources of gravitational radiation” in Gravitational Wave Data Analysis, eds. B. F. Schutz, Kluwer Academic Publisher (1987)
- [7] P. Astone, S. Frasca “Robust estimation of the parameters of a disturbed non-stationary Gaussian process” arXiv:0905.2572. Presented to the GWDAW13 workshop, Jan 2009
- [8] P. Jaranowski, A. Krolak, “Search for gravitational waves from known pulsars using \mathcal{F} and \mathcal{G} statistics” <http://xxx.lanl.gov/abs/1004.0324>